ADVANCED FUNCTIONAL MATERIALS

FULL PAPER

DOI: 10.1002/adfm.200600973

Observation of Structural and Conductance Transition of Rotaxane Molecules at a Submolecular Scale**

By *Min Feng*, *Li Gao*, *Shixuan Du*, *Zhitao Deng*, *Zhihai Cheng*, *Wei Ji*, *Deqing Zhang*, *Xuefeng Guo*, *Xiao Lin*, *Lifeng Chi*, *Daoben Zhu*, *Harald Fuchs*, and *Hongjun Gao**

Rotaxane molecules have attracted considerable interest because of their good performance in both molecular electronic devices and nanoscale data-storage media. Low-temperature scanning tunneling microscopy is used to investigate the structure and conductance of single H2 rotaxane molecules on a buffer-layered Au(111) substrate at 77 K. It is demonstrated that the conductance switching in rotaxane-based, solid-state devices is an inherent property of the rotaxane molecules. These results provide evidence that the conductance switching might arise from the movement of the cyclobis(paraquat-*p*-phenylene) ring along the rod section of the dumbbell-shaped backbone of the rotaxane molecule.

1. Introduction

Scanning tunneling microscopy (STM) has been widely used to study the growth, structures, and electronic states, and to induce motions, of molecules.[1–24] It has also been used to induce conductance transitions aimed at achieving a nonvolatile, nanoscale data-storage medium.[8–13,25] Rotaxane-based molecules in particular offer significant potential for use in functional molecular electronic devices.[26–33] Rotaxanes themselves have shown considerable potential for applications in functional molecular electronic devices[26–27,29–31,33–36] and nanoscale data recording.[37] Exploring the mechanism of conductance switching in rotaxane-based solid-state devices has attracted considerable interest in recent years. Structural bistability of some rotaxane molecules has been observed in solution phase. These molecules contain a π-electron-deficient ring component that encircles a dumbbell-shaped component incorporating two π-electron-rich recognition sites in its rod section and terminated by bulky "stoppers". The ring component, cyclobis(paraquat-*p*-phenylene) ($CBPQT^{4+}$), can move back and forth between the two π-electron-rich recognition sites on the dumbbell-shaped backbone in response to external stimuli, resulting in the switching between two stable structures. Switching between the two stable structures can lead to switching of conductance, which makes rotaxane molecules potential candidates for ultrahigh-density information storage. However, in all practical applications, the rotaxane molecules would have to be in the solid state. Although the conductance switching of rotaxane is well defined in solution, it is still ambiguous in solid-state form.[28,38–41]

In this paper, we show that the structural bistability exists for single H2 rotaxane molecules on a buffer-layered solid surface and that the structure transition is accompanied by conductance switching at 77 K. We also achieved the reversible writing and erasing of information dots on solid-state H2 rotaxane films at room temperature. STM is employed in our experiments as it has been proved to be a powerful tool not only for manipulating intramolecular structure and local measurement of electronic states[1–18] but also for inducing local conductance transition on functional thin films to realize nanoscale recording.[8–13,25] Ab initio and molecular mechanics (MM) calculations are employed to explain the transition mechanism.

2. Results and Discussion

2.1. Conductance Switching for Single Rotaxane Molecules

2.1.1. Sample Preparation

A sample of a single rotaxane molecules for STM study was prepared on a buffer-layered Au(111) surface. Our experimental objective was to verify which is responsible for the conductance switching in rotaxane-based solid-state devices, the interface effect or the inherent property of rotaxane molecules. In order to investigate the inherent property of rotaxane mole-

[*] Prof. H.-J. Gao, Dr. M. Feng, Dr. L. Gao, Dr. S. X. Du, Z. T. Deng, Z. H. Cheng, W. Ji, Dr. X. Lin
Institute of Physics, Chinese Academy of Sciences
PO Box 603, Beijing 100080 (P.R. China)
E-mail: hjgao@aphy.iphy.ac.cn
Prof. D. Q. Zhang, Dr. X. F. Guo, Prof. D. B. Zhu
Institute of Chemistry, Chinese Academy of Sciences
Beijing 100080 (P.R. China)
Prof. L. F. Chi, Prof. H. Fuchs
Physikalisches Institute/CeNTech, Universität Münster
48149 Münster (Germany)

[**] This project is partially supported by the Natural Scientific Foundation of China, National 973 and 863 projects of China, the Supercomputing Center, NCIC, CAS, and the Shanghai Supercomputer Center. Work in Münster was supported by the Ministry of Science and Research (MWF), Nordrhein–Westfalen (Germany). Supporting Information is available online from Wiley InterScience or from the author.

cules, the interaction between the rotaxane molecule and the gold substrate should be effectively screened.[42,43] In our experiments, an insulating buffer layer is self-assembled between the molecules and the substrate, which effectively weakens the interaction between the rotaxane molecules and the gold. A small molecule, CH_2Cl_2, was used as the insulating buffer-layer material because CH_2Cl_2 molecules have great ability to self-assemble on the Au(111) surface, and it is also a good solvent for rotaxane molecules.

High self-assembly ability was observed for CH_2Cl_2 molecules on the Au(111) surface in our experiments. The self-assembled CH_2Cl_2 monolayer was prepared by dropping CH_2Cl_2 solvent onto the clean Au(111) surface in nitrogen atmosphere at room temperature. Thereafter, the sample was annealed at 330 K in ultrahigh vacuum (UHV). Subsequent STM observations showed high-quality self-assembled monolayer (SAMs) had been achieved, as shown in Figure 1a. Auger electron spectroscopy measurements on the SAM showed the signature of Cl,[44,45] but no signals for O and N, see Figure 1c and d, which confirms that the observed self-assembled structures are formed of CH_2Cl_2 molecules. Figure 1a shows that the CH_2Cl_2 molecules arranged into stripes.

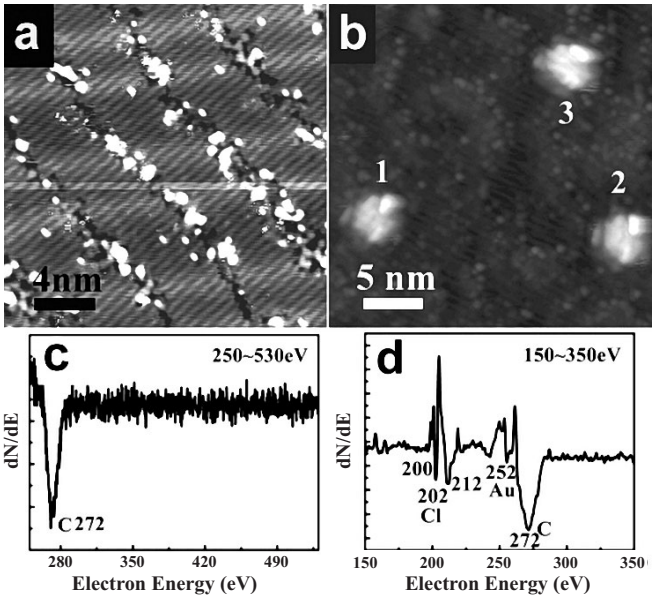

Figure 1. a) STM image (20 nm × 20 nm) of CH_2Cl_2 self-assembled monolayer after annealing at 85 °C. Bias voltage $U = -1.3$ V, current $I = 0.08$ nA. b) STM image (30 nm × 30 nm) of rotaxane molecules on the CH_2Cl_2 self-assembled monolayer. Scanning parameters: $U = -1.2$ V, $I = 0.03$ nA. c) Auger electron spectroscopy (250–530 eV) of CH_2Cl_2/Au(111) sample. The C element was detected. The O and N elements were not detected. d) Auger electron spectroscopy (150–350 eV) of CH_2Cl_2/Au(111) sample. The Cl element was detected.

To prepare the sample of isolated H2 rotaxane molecules on a surface, we first dissolved the rotaxane molecules in CH_2Cl_2 solution, with a molarity of 8×10^{-6} mol L^{-1}, then placed several drops of the rotaxane/CH_2Cl_2 solution onto a clean Au(111) surface that was prepared by using the standard UHV method, i.e., repeated cycles of Ar^+ sputtering and annealing.[46] To check whether the rotaxane molecules were isolated from the gold substrate by the SAM using this preparation method, voltage pulses were used to remove the rotaxane molecules from their adsorption sites. Subsequent STM images of the same area showed that there was no defect in the SAM at the original molecular adsorption sites, which confirms that the rotaxane molecules were actually adsorbed on the SAM.

2.1.2. STM Images of Single Rotaxane Molecules

STM observations show that isolated rotaxane molecules are dispersed on the self-assembled CH_2Cl_2 monolayer (see Fig. 1b). Various molecular conformations have been observed in our STM experiments. In Figure 1b, molecules 1 and 2 have the same conformation, while molecule 3 has a different conformation. We observed 25 different conformations in total for the rotaxane molecules, see Figure 2a. According to our STM experiments, when the distance between two adjacent molecules is less than 5 nm, the two molecules tend to take on the same conformation. Therefore, molecules influence the conformation of adjacent molecules only at small spacing.

2.1.3. Conductance Switching of Single Rotaxane Molecules

Scanning tunneling spectroscopy (current–voltage (*I–V*) curves) measurements have been conducted on the adsorbed rotaxane molecules. As STM is capable of high-spatial-resolution measurements, we collected *I–V* data at several different points on a single rotaxane molecule, see Figure 2b. Our measurements indicate that there is little difference between *I–V* curves across the molecule, which indicates that the electron tunneling is occurring via the whole molecule. As the molecular conformation may have an influence on the *I–V* properties at the single-molecule scale,[47] we also performed scanning tunneling spectroscopy measurements on H2 molecules with different conformations. Numerous measurements showed that the molecular conformation has no obvious effect on *I–V* curves. There is a zero-conductance gap of ca. 1.8 eV for the as-deposited rotaxane molecules.

A structure/conductance transition in a single rotaxane molecule was observed by varying the polarity of the voltage bias applied between the tip and the sample in the STM experiments. Figure 3a–d shows sequential STM images with the polarity of the voltage reversed bias between one scan and the next, together with the corresponding measured *I–V* curves (see Fig. 3e). The change of the scanning voltage from –1.3 V to 1.3 V led to changes in both the molecular STM image and the *I–V* curve. When the voltage bias changes from +1.3 V back to –1.3 V, both the molecular STM image and the *I–V* curve revert to their original states. This process was reversible and repeatable in our experiments.

The above results, however, are not enough to make the argument that any structural transition occurred and induced conductance switching for single rotaxane molecules. Firstly, the observed change in the molecular STM images may have been induced by the difference between the spatial distribution of the lowest unoccupied molecular orbital (LUMO) and

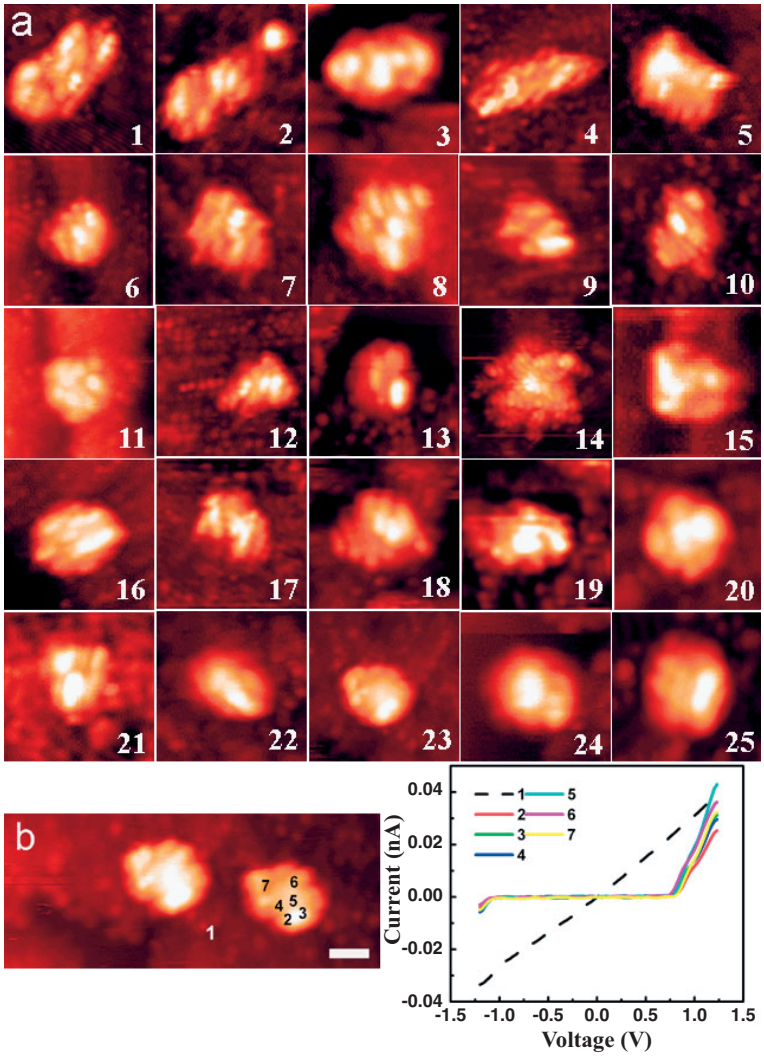

Figure 2. a) STM images showing 25 types of molecular conformations for individual rotaxane molecules in our STM observation. Scanning parameters: $U = -1.3$ V, $I = 0.03$ nA. Image size: 10 nm × 10 nm for 1–17; 8 nm × 8 nm for 18 and 19; 7 nm × 7 nm for 20; 6 nm × 6 nm for 21–23; 5 nm × 5 nm for 24; 4 nm × 4 nm for 25. It is obvious that the molecular apparent size varies greatly with its conformation. b) *I–V* curves at different points of single rotaxane molecule are roughly the same. Scale bar is 2 nm. Both the STM image and *I–V* curves are recorded at 77 K.

the highest occupied molecular orbital (HOMO). Secondly, the difference in *I–V* curves may have been induced by the difference in the tip–sample distance under different voltages.[48–51]

The sequential STM images shown in Figure 4a–e, however, exclude the possibility of the above two doubts. Figure 4a and b show that when the voltage bias changes from –1.3 V to +1.3 V, the molecular image and the *I–V* curve are not immediately changed. The subsequent STM image, Figure 4c, captures the instant of change for the molecular image. Figure 4d shows that both the structure and the *I–V* curves have changed. Analysis of the process from Figure 4a–d produces two conclusions. First, the change of the molecular STM image is induced by the structural change instead of the difference between LUMO and HOMO imaging. Second, the change in *I–V* curves represents the conductance switching, and is not an experimental artifact. Finally, we changed the bias voltage back to the initial negative polarity, and the molecular image returned precisely to its initial state (Fig. 4e), with the *I–V* curves corresponding to the initial low-conductivity state. The observed correlation between structural change and conductance change is reversible and repeatable. This suggests that the conductance transition is induced by the intramolecular structural transition.

In our STM experiments, not all of the molecules on the surface showed structure/conductance transition. For the present, we are not sure whether the conformation is responsible for this, considering the following two facts. First, it is quite difficult to identify the precise conformations of the molecules on the surface according to the STM images alone. Second, as the rotaxane molecules were dispersed on the substrate, interaction between the molecules and the substrate might have influenced the switching properties of the molecules. In our STM observations, we have observed an ordered layer of the solvent molecule (CH_2Cl_2) co-existing with the rotaxane molecules on the Au substrate. This ordered layer isolates the molecules from the Au substrate and decreases the interaction between the rotaxanes and the Au. However, experimentally, different molecular conformations generally correspond to different molecular appearances in the STM images, and we show some experimental data in Figure 3f. We performed transition experiments on twelve molecules, of which eight (1–8 in Fig. 3f) showed structure/conductance transition, while four (9–12 in Fig. 3f) did not. Molecules 1 and 3 have the same molecular conformation, as do molecules 6 and 11. According to these experimental results, it is not safe to say that conductance switching can always be observed for one molecular conformation and never for another. We can only say that the molecular conformation influences the probability of conductance switching.

In our STM experiments, the structure/conductance switching was realized by switching the polarity of sample–tip voltage bias between –1.3 V and +1.3 V. The switching is a sudden incident, as shown in Figure 3c. In some cases, for example, #2 and #4 in Figure 3h, we captured the switching moment because the switching occurred while STM tip was scanning over the molecule, also seen in Figure 4c. In this case, we know exactly what the time interval is between the polarity change and the structure/conductance switching. However, in the other cases, #1 and #3 in Figure 3h, we did not capture the switching moment because the switching occurred while STM tip was scanning over the SAM surface rather than over the molecules. In this case, we can only give a range for the time interval between the polarity change and the structure/conductance switching. Figure 3g shows statistics for the above time interval for molecules 1–8 in Figure 3f.

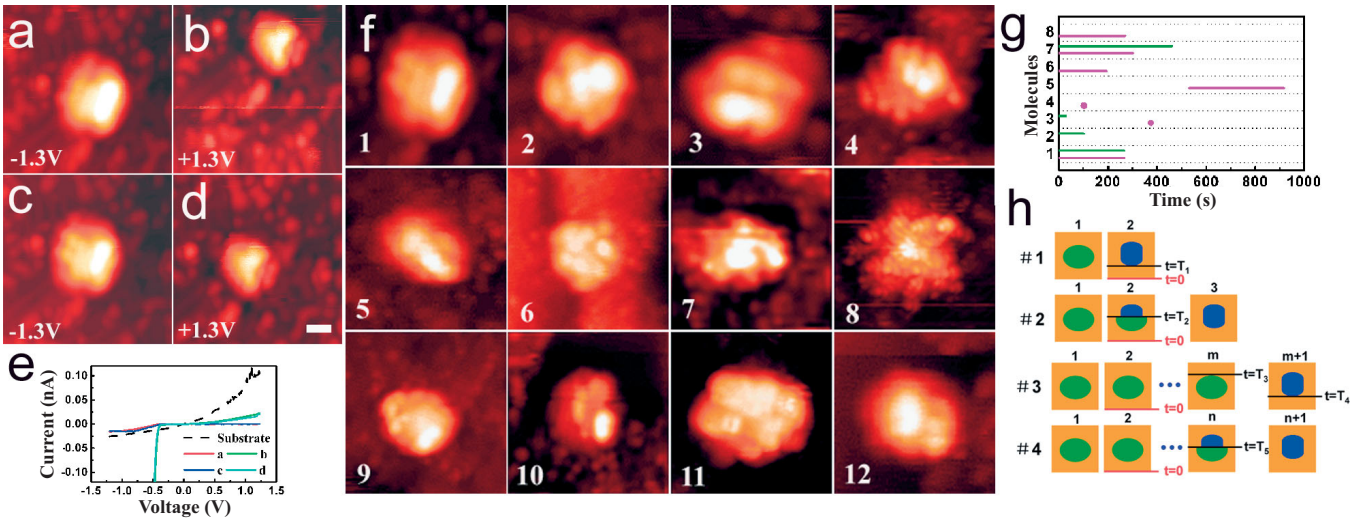

Figure 3. a–d) Reversible conductance transitions induced sequentially in an individual rotaxane molecule by the STM field. STM images show different but consistent forms on sequentially reversing the bias polarity. The scale bar is 1 nm. e) *I–V* characteristics. f) STM images of twelve different molecules. g) The time intervals between the polarity change and structure/conductance switching for 1–8 molecules in (f). Magenta represents the time interval between polarity change from –1.3 V to +1.3 V and the structure/conductance switching. Olive represents the time interval between polarity change from +1.3 V to –1.3 V and the structure/conductance switching. Line represents switching occurred at a moment during that time range. Dot represents switching occurred at that moment. h) The sketch map for the statistics in (g). Four cases (#1, #2, #3, and #4) are listed. When $t = 0$, the polarity of the scanning voltage is reversed. For the case of #1, the transition moment lies between $0 \sim T_1$; For the case of #2, the transition moment is at $t = T_2$; For the case of #3, the transition moment lies between $T_3 \sim T_4$; For the case of #4, the transition moment is at $t = T_5$.

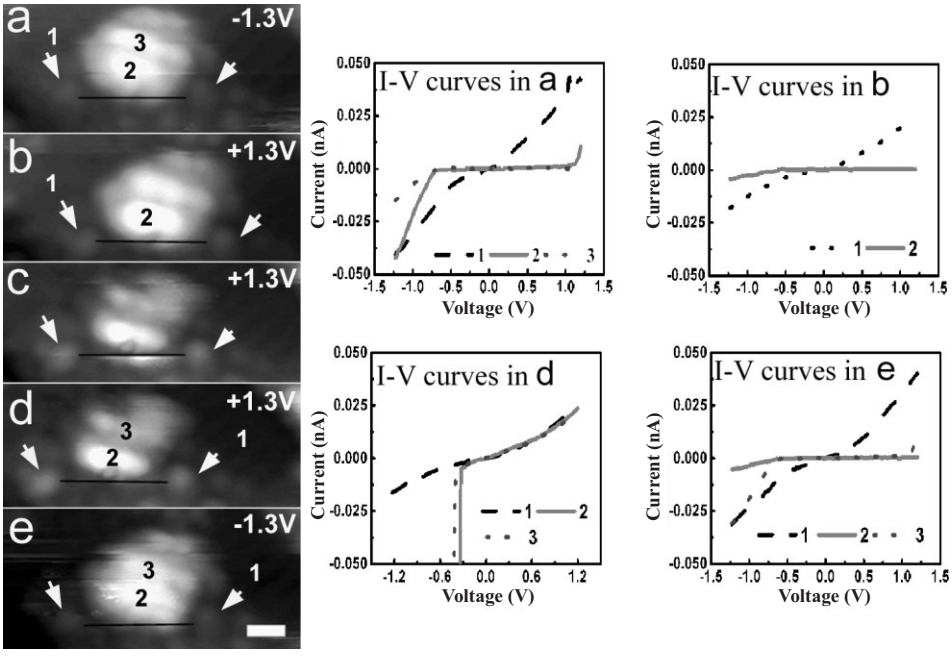

Figure 4. A sequence of STM images of a single rotaxane molecule showing a reversible conductance transition correlated with a change in molecular structure. a,b) STM images obtained with changed bias polarity show similar image, indicating similar HOMO and LUMO distribution. c) As the tip approaches the molecule a sudden structure transition induces the molecule to jump across the substrate. d) The molecule stays in this new position for the next scan. e) It recovers its original structure perfectly when the voltage bias is set to its original polarity. The green lines and circles mark features on the substrate for reference; the scale bar size is 1 nm. *I–V* characteristics show that the conformation change is associated with a transition to a high-conductance state. Numbers on the images represent positions of the *I–V* measurements.

2.2. Understanding the Mechanism of Conductance Switching

Stoddart and co-workers pointed out that the conductivity of rotaxane molecules is mainly determined by the $CBPQT^{4+}$ and tetrathiafulvalene (TTF) and 1,5-dioxynaphthalene (DNP) groups (the recognition sites), and that the electron tunneling occurs via the whole molecule if these groups are crowded together.[34–36] *I–V* measurements taken at different points of the molecule, as shown in Figure 2b, found that the electrons tunnel through the whole molecule. Therefore, the $CBPQT^{4+}$, TTF, and DNP groups are crowded together, according to previous theoretical prediction. It was also predicted that the conductance switching is induced by the movement of the ring component $CBPQT^{4+}$ between the DNP and TTF recognition sites, when activated by an external stimulus. In STM experiments, the external stimulus is the inelastic electron tunneling process that transfers the energy of inelastic tunneling electrons to the ring component.

There are two factors that influence the structure/conductance transition of single rotaxane molecule, the underlying CH_2Cl_2 insulating layer and the molecular conformation. On one hand, the CH_2Cl_2 buffer layer effectively weakens the coupling between the Au substrate and the rotaxane molecules. Experiments on rotaxane molecules directly adsorbed on the Au substrate all failed to observe structure/conductance transition, which is ascribed to the strong bonding between the Au substrate and the molecules (e.g., the S atoms in the rotaxane molecule). Hence, the existence of the CH_2Cl_2 buffer layer is a prerequisite for conductance switching. On the other hand, not all rotaxane molecules isolated by the buffer layer show structure/conductance transitions, which means molecular conformation is another crucial factor. Although 25 different molecular conformations have been observed in our STM experiments, none of them is a fully extended structure, as shown in Figure 5a. To identify the molecular conformation of a free rotaxane molecule, we carried out fully optimized density functional theory (DFT) calculations and classical force-field calculations. Owing to numerical limitations and the size of the molecule, we initially built two simplified models by removing the two large stoppers and the four PF_6^- anions from the rotaxane molecule—see 1 and 2 in Figure 5b. Structure optimization was performed by using the Gaussian 03 program package at the DFT-B3LYP(3-21G) level for the two models.[52–55] Whether the CBPQT is at the TTF or DNP sites, the simplified backbone is not linear but curved, see 1 and 2 in Figure 5b. In addition, structure optimization for the entire rotaxane molecule was carried out using molecular mechanics with an MM^+ force field.[56] This result also showed a curved backbone (see 3 in Fig. 5b). These curved structures indicate that, for rotaxane molecules, the backbone cannot form a linear molecule because of the two stoppers and the $CBPQT^{4+}$ component. The curved structure provides more space for $CBPQT^{4+}$ to move between TTF and DNP. Besides this, the calculation results explain the ellipsoidal appearance of the rotaxane molecules on CH_2Cl_2/Au(111), and also why the rotaxane molecule adopts so many different conformations. Rotaxane is a large, flexible molecule that can adopt many possible molecular conformation, some of which facilitate the movement of the $CBPQT^{4+}$ in the case of individual rotaxane molecules on a solid surface. So the molecular conformation influences the probability of conductance switching.

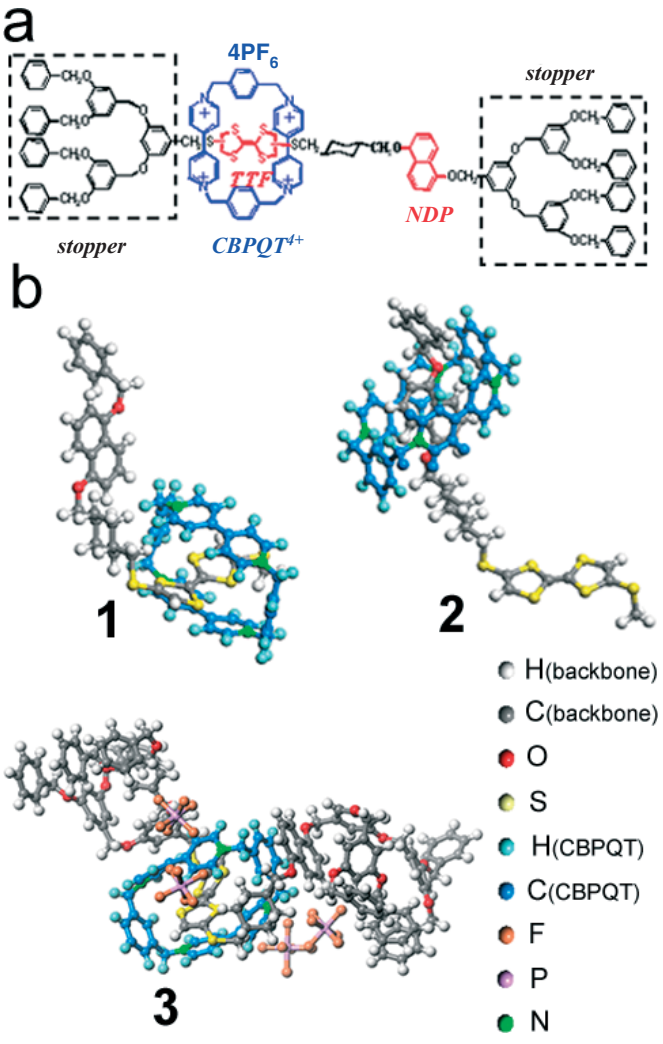

Figure 5. a) Structure model of the rotaxane molecule. The end parts enclosed by dashed line are the stoppers preventing the CBPQT4+ disengaging from the molecular backbone. The CBPQT4+ is colored in blue. The tetrathiafulvalene (TTF) and 1,5-dioxynaphthalene (DNP) are colored in red. b) Fully optimized structure of a simplified model for molecule with the CBPQT ring positioned over the TTF group (1) and over the DNP group (2). 3 is the result of molecular mechanics calculation of the entire molecule. All calculations confirm a curved conformation for the rotaxane molecule.

2.3. Conductance Transition in Thin Films

Beyond the single-molecular level, we have also investigated the possibility of inducing conductance transitions in rotaxane thin films prepared by using the Langmuir–Blodgett technique. Using the STM tip, we achieved writable, erasable, and rewritable recording by applying different-polarity voltage pulses. The marks could be created reproducibly with voltage pulses of around 2.0 V ranging from 0.1 to 10 ms in duration, as in the

case of H1 rotaxane molecules.[25] For the H2-molecule thin films, however, the recorded marks could be erased, rewritten, and re-erased on the same site. Throughout this entire process the marks remained at about 3 nm in size and were stable in air for more than four weeks. The marks are also directly observable in current images obtained by conductive contact AFM imaging, but are invisible in the topographic image, which shows that the marks are indeed induced by conductance transitions. Micro-Raman spectra of the rotaxane films before and after the transition from the low-conductance state to the high-conductance state also found that the conductance transition is caused by the intramolecular motion of the $CBPQT^{4+}$, just as in the case of single rotaxane molecules.[57]

3. Conclusions

The structural and conductance transition of a single H2 molecule has been directly observed using low temperature scanning tunneling microscopy at 77 K. Our results show that the conductance switching of the rotaxane molecule is attributable to the inherent property of the molecule, and caused by an intramolecular structural transition.

Received: October 17, 2006
Revised: February 9, 2007

[1] J. A. Stroscio, D. M. Eigler, *Science* **1991**, *254*, 1319.
[2] D. M. Eigler, C. P. Lutz, W. E. Rudge, *Nature* **1991**, *352*, 600.
[3] A. Sato, Y. Tsukamoto, *Nature* **1993**, *363*, 431.
[4] J. K. Gimzewski, C. Joachim, *Science* **1999**, *283*, 1683.
[5] D. I. Gittins, D. Bethell, D. J. Schiffrin, R. J. Nichols, *Nature* **2000**, *408*, 67.
[6] Z. J. Donhauser, B. A. Mantooth, K. F. Kelly, L. A. Bumm, J. D. Monnell, J. J. Stapleton, D. W. Price, Jr., A. M. Rawlett, D. L. Allara, J. M. Tour, P. S. Weiss, *Science* **2001**, *292*, 2303.
[7] W. J. Liang, M. P. Shores, M. Bockrath, J. R. Long, H. Park, *Nature* **2002**, *417*, 725.
[8] H. J. Gao, K. Sohlberg, Z. Q. Xue, H. Y. Chen, S. M. Hou, L. P. Ma, X. W. Fang, S. J. Pang, S. J. Pennycook, *Phys. Rev. Lett.* **2000**, *84*, 1780.
[9] D. X. Shi, Y. L. Song, H. X. Zhang, P. Jiang, S. T. He, S. S. Xie, S. J. Pang, H. J. Gao, *Appl. Phys. Lett.* **2000**, *77*, 3203.
[10] D. X. Shi, Y. L. Song, D. B. Zhu, H. X. Zhang, S. S. Xie, S. J. Pang, H.-J. Gao, *Adv. Mater.* **2001**, *13*, 1103.
[11] L. P. Ma, Y. L. Song, H. J. Gao, W. B. Zhao, H. Y. Chen, Z. Q. Xue, S. J. Pang, *Appl. Phys. Lett.* **1996**, *69*, 3752.
[12] L. P. Ma, J. Liu, Y. Yang, *Appl. Phys. Lett.* **2002**, *80*, 2997.
[13] K. Yano, M. Kyogaku, R. Kuroda, Y. Shimada, S. Shido, H. Matsuda, K. Takimoto, O. Albrecht, K. Eguchi, T. Nakagiri, *Appl. Phys. Lett.* **1996**, *68*, 188.
[14] A. Bandyopadhyay, A. J. Pal, *Appl. Phys. Lett.* **2003**, *82*, 1215.
[15] V. Bermudez, N. Capron, T. Gase, F. G. Gatti, F. Kajzar, D. A. Leigh, F. Zerbetto, S. Zhang, *Nature* **2000**, *406*, 608.
[16] H. Yanagi, K. Lkuta, H. Mukai, T. Shibutani, *Nano Lett.* **2002**, *2*, 951.
[17] B. C. Stipe, M. A. Rezaei, W. Ho, *Science* **1998**, *279*, 1907.
[18] T. A. Jung, R. R. Schlittler, J. K. Gimzewski, H. Tang, C. Joachim, *Science* **1996**, *271*, 181.
[19] J. V. Barth, G. Costantini, K. Kern, *Nature* **2005**, *437*, 671.
[20] H. Tian, Q. C. Wang, *Chem. Soc. Rev.* **2006**, *35*, 361.
[21] Z. T. Deng, H. Lin, W. Ji, L. Gao, X. Lin, Z. H. Cheng, X. B. He, J. L. Lu, D. X. Shi, W. A. Hofer, H.-J. Gao, *Phys. Rev. Lett.* **2006**, *96*, 156 102.
[22] D. X. Shi, W. Ji, X. Lin, X. B. He, J. C. Lian, L. Gao, J. M. Cai, H. Lin, S. X. Du, F. Lin, C. Seidel, L. F. Chi, W. A. Hofer, H. Fuchs, H.-J. Gao, *Phys. Rev. Lett.* **2006**, *96*, 226 101.
[23] S. X. Du, H. J. Gao, C. Seidel, L. Tsetseris, W. Ji, H. Kopf, L. F. Chi, H. Fuchs, S. J. Pennycook, S. T. Pantelides, *Phys. Rev. Lett.* **2006**, *97*, 156 105.
[24] Y. L. Wang, W. Ji, D. X. Shi, S. X. Du, C. Seidel, Y. G. Ma, H.-J. Gao, L. F. Chi, H. Fuchs, *Phys. Rev. B* **2004**, *69*, 075 408.
[25] M. Feng, X. F. Guo, X. Lin, X. B. He, W. Ji, S. X. Du, D. Q. Zhang, D. B. Zhu, H. J. Gao, *J. Am. Chem. Soc.* **2005**, *127*, 15 338.
[26] R. A. Bissell, E. Cordova, A. E. Kaifer, J. F. Stoddart, *Nature* **1994**, *369*, 133.
[27] C. P. Collier, E. W. Wong, M. Belohradsky, F. M. Raymo, J. F. Stoddart, P. J. Kuekes, R. S. Williams, J. R. Heath, *Science* **1999**, *285*, 391.
[28] C. P. Collier, G. Mattersteig, E. W. Wong, Y. Luo, K. Beverly, J. Sampaio, F. M. Raymo, J. F. Stoddart, J. R. Heath, *Science* **2000**, *289*, 1172.
[29] Y. Luo, C. P. Collier, J. O. Jeppesen, K. A. Nielsen, E. DeIonno, G. Ho, J. Perkins, H.-R. Tseng, T. Yamamoto, J. F. Stoddart, J. R. Heath, *ChemPhysChem* **2002**, *3*, 519.
[30] D. R. Stewart, D. A. A. Ohlberg, P. A. Beck, R. S. Williams, J. F. Stoddart, *Nano Lett.* **2004**, *4*, 133.
[31] H. B. Yu, Y. Luo, K. Beverly, J. F. Stoddart, H. Tseng, J. R. Heath, *Angew. Chem. Int. Ed.* **2003**, *42*, 5706.
[32] A. Bandyopadhyay, A. J. Pal, *Appl. Phys. Lett.* **2003**, *82*, 1215.
[33] C. Joachim, J. K. Gimzewski, and A. Aviram, *Nature* **2000**, *408*, 541.
[34] P. M. Mendes, A. H. Flood, J. F. Stoddart, *Appl. Phys. A* **2005**, *80*, 1197.
[35] S. S. Jang, Y. H. Jang, Y.-H. Kim, W. A. Goddard III, A. H. Flood, B. W. Laursen, H.-R. Tseng, J. F. Stoddart, J. O. Jeppesen, J. W. Choi, D. W. Steuerman, E. DeIonno, J. R. Heath, *J. Am. Chem. Soc.* **2005**, *127*, 1563.
[36] A. H. Flood, A. J. Peters, S. A. Vignon, D. W. Steuerman, H.-R. Tseng, S. Kang, J. R. Heath, J. F. Stoddart, *Chem. Eur. J.* **2004**, *10*, 6558.
[37] M. Cavallini, F. Biscarini, S. León, F. Zerbetto, G. Bottari, D. A. Leigh, *Science* **2003**, *299*, 531.
[38] C. P. Collier, J. O. Jeppesen, Y. Luo, J. Perkins, E. W. Wong, J. R. Heath, J. F. Stoddart, *J. Am. Chem. Soc.* **2001**, *123*, 12 632.
[39] Y. H. Jang, S. Hwang, Y. H. Kim, S. S. Jang, W. A. Goddard, III, *J. Am. Chem. Soc.* **2004**, *126*, 12 636.
[40] W. Q. Deng, R. P. Muller, W. A. Goddard, III, *J. Am. Chem. Soc.* **2004**, *126*, 13 562.
[41] R. F. Service, *Science* **2003**, *302*, 556.
[42] J. Repp, G. Meyer, *Phys. Rev. Lett.* **2005**, *94*, 026 803.
[43] J. Weissenrieder, S. Kaya, J.-L. Lu, H.-J. Gao, S. Shaikhutdinov, H.-J. Freund, M. Sierka, T. K. Todorova, J. Sauer, *Phys. Rev. Lett.* **2005**, *95*, 076 103.
[44] E. J. Aitken, M. K. Bahl, K. D. Bomben, J. K. Gimzewski, G. S. Nolan, T. D. Thomas, *J. Am. Chem. Soc.* **1980**, *102*, 4873.
[45] L. E. Davis, N. C. MacDonald, P. W. Palmberg, G. E. Riach, R. E. Weber, *Handbook of Auger Electron Spectroscopy*, 2nd ed., Perkin–Elmer, Eden Prairie, MN **1976**.
[46] R. G. Musket, W. Mclean, C. A. Colmenares, D. M. Makowiecki, W. J. Siekhaus, *Appl. Surf. Sci. (1977–1985)* **1982**, *10*, 143.
[47] Y. B. Hu, Y. Zhu, H. J. Gao, H. Guo, *Phys. Rev. Lett.* **2005**, *95*, 156 803.
[48] S. Datta, W. Tian, S. Hong, R. Reifenberger, J. I. Henderson, C. P. Kubiak, *Phys. Rev. Lett.* **1997**, *79*, 2530.
[49] A. P. Labonté, *Ph.D. Thesis*, Purdue University, West Lafayette, IN **2002**.
[50] W. Tian, S. Datta, S. Hong, R. G. Reifenberger, J. I. Henderson, C. P. Kubiak, *Phys. E* **1997**, *1*, 304.
[51] W. Tian, S. Datta, S. Hong, R. Reifenberger, J. I. Henderson, C. P. Kubiak, *J. Chem. Phys.* **1998**, *109*, 2874.
[52] M. J. Frisch, G. W. Trucks, H. B. Schlegel, G. E. Scuseria, M. A. Robb, J. R. Cheeseman, J. A. Montgomery, Jr., T. Vreven, K. N. Ku-

din, J. C. Burant, J. M. Millam, S. S. Iyengar, J. Tomasi, V. Barone, B. Mennucci, M. Cossi, G. Scalmani, N. Rega, G. A. Petersson, H. Nakatsuji, M. Hada, M. Ehara, K. Toyota, R. Fukuda, J. Hasegawa, M. Ishida, T. Nakajima, Y. Honda, O. Kitao, H. Nakai, M. Klene, X. Li, J. E. Knox, H. P. Hratchian, J. B. Cross, C. Adamo, J. Jaramillo, R. Gomperts, R. E. Stratmann, O. Yazyev, A. J. Austin, R. Cammi, C. Pomelli, J. W. Ochterski, P. Y. Ayala, K. Morokuma, G. A. Voth, P. Salvador, J. J. Dannenberg, V. G. Zakrzewski, S. Dapprich, A. D. Daniels, M. C. Strain, O. Farkas, D. K. Malick, A. D. Rabuck, K. Raghavachari, J. B. Foresman, J. V. Ortiz, Q. Cui, A. G. Baboul, S. Clifford, J. Cioslowski, B. B. Stefanov, G. Liu, A. Liashenko, P. Piskorz, I. Komaromi, R. L. Martin, D. J. Fox, T. Keith, M. A. Al-Laham, C. Y. Peng, A. Nanayakkara, M. Challacombe, P. M. W. Gill, B. Johnson, W. Chen, M. W. Wong, C. Gonzalez, J. A. Pople, *Gaussian 03*, Revision C.02, Gaussian, Inc., Wallingford, CT **2004**.

[53] J. S. Binkley, J. A. Pople, W. J. Hehre, *J. Am. Chem. Soc.* **1980**, *102*, 939.

[54] A. D. Becke, *Phys. Rev. A* **1988**, *38*, 3098.

[55] C. Lee, W. Yang, R. G. Parr, *Phys. Rev. B* **1988**, *37*, 785.

[56] N. L. Allinger, *J. Am. Chem. Soc.* **1977**, *99*, 8127

[57] M. Feng, L. Gao, Z. T. Deng, W. Ji, S. X. Du, X. F. Guo, D. Q. Zhang, D. B. Zhu, H.-J. Gao, *J. Am. Chem. Soc.* **2007**, *129*, 2204.